Photocatalytic Hydrogen Evolution from Pure Water Using a New Sm_2GaTaO_7 Advanced Compound

Miguel A. Ruiz-Gómez[1,2], Leticia M. Torres-Martínez[1,*], M. Z. Figueroa-Torres[1], Edgar Moctezuma[2], Isaías Juárez-Ramírez[1]
[1]Universidad Autónoma de Nuevo León, UANL, Facultad de Ingeniería Civil, Departamento de Ecomateriales y Energía, Av. Universidad S/N Ciudad Universitaria San Nicolás de los Garza Nuevo León, C.P. 66451 México
[2]Facultad de Ciencias Químicas, Universidad Autónoma de San Luis Potosí, Av. Manuel Nava #6, 78290 San Luis Potosí, S.L.P., México
*Tel: 81 83521983 ext. 222, fax 81 83760477, mail: lettorresg@yahoo.com

ABSTRACT

Overall water splitting to produce hydrogen over a semiconductor photocatalyst is a promising process for clean and sustainable hydrogen production. In this work, a new compound Sm_2GaTaO_7 was successfully synthesized by a conventional solid state reaction. RuO_2 nanoparticles were loaded as cocatalyst onto Sm_2GaTaO_7 surface. X-ray powder diffraction and Rietveld refinement characterization results revealed that Sm_2GaTaO_7 crystallized in the monoclinic system with space group C2/c. The energy band gap (*Eg*) was calculated by Kubelka-Munk formula, obtaining a value in the order of 4.1 eV. By scanning electron microscopy and nitrogen physisorption analysis, it was observed that material presents particle size around 2-3 μm and a specific surface area of 0.5 $m^2 g^{-1}$. The photocatalytic water splitting reaction results revealed that Sm_2GaTaO_7 was able to produce hydrogen from pure water. The hydrogen production activity was enhanced by using the optimal RuO_2 amount, which exceeded 2.4 times the production of pure Sm_2GaTaO_7.

1. Introduction

Actually, hydrogen (H_2) has received special attention as a next-generation energy carrier. H_2 is widely considered to be the future clean energy in many applications, such as environmentally friendly vehicles, domestic heating, and stationary power generation. Photocatalytic water splitting using semiconductor oxide is one of the most promising technologies for sustainable and clean hydrogen production; this is because H_2 could be obtained directly from abundant and renewable sources such as water and solar light [1-5].

Photocatalysts materials that include in their structure cations with d^0 electronic configuration like Ti^{4+}, Zr^{4+}, Nb^{5+} and Ta^5 have been widely studied and showed potential activity for water splitting into H_2 and O_2 [1,4,6-8]. On the other hand, it has been reported that some metal oxides consisting of cations with d^{10} electronic configuration such as Ga^{3+}, In^{3+}, Ge^{4+}, Sn^{4+} and Sb^{5+} are also attractive materials for this reaction [9-11]. Density functional theory results (DFT) revealed that the conduction band of d^{10} metal oxides present a large dispersion which allows higher mobility of the photoexcited electrons than d^0 transition metals [11]. However, pyrochlore-type mixed oxides Sm_2InTaO_7 and Sm_2InNbO_7 that combine cations with 4f-d^{10}-d^0 configuration showed much higher activity for H_2 evolution when compared to $Sm_2Zr_2O_7$ and $InNbO_4$ with 4f-d^0 and d^{10}-d^0 electronic configuration respectively [12,13]. Moreover, some investigations have found that crystalline structure arrangement, particularly, the formation of distorted octahedral units is an important factor to improve the H_2 evolution using 4f, d^{10} and d^0 mixed metal oxides [12-15].

Other way to improve the photocatalytic water splitting reaction is through a surface modification loading Pt, NiO and RuO_2 nanoparticles as cocatalysts. Principally, the cocatalyst materials suppress the electron-hole recombination and generate active sites for gas evolution [1,4].

Among metal oxides with d^{10} configuration, Ga_2O_3 is photocatalytically active for the water splitting reaction, even without loading a cocatalyst [4]. Based on above consideration, this paper is focused on the synthesis by solid state reaction of a new compound, Sm_2GaTaO_7. Their photocatalytic activity for water splitting reaction to produce hydrogen was studied. The hydrogen evolution results were explained in terms of the crystalline structure and the effect of loading RuO_2 nanoparticles.

2. Experimental

2.1 Synthesis by solid state reaction

Sm_2GaTaO_7 was synthesized by solid state reaction using Sm_2O_3, Ga_2O_3 and Ta_2O_5 (Aldrich purity > 99.9 %) as starting materials. The powders were dried before the synthesis at 200ºC for 4 hours. Then, stoichiometric amounts of each reactant were perfectly mixed with acetone in an agate mortar. The mixture was grinding until complete evaporation of acetone. Then, the mixture was placed into a platinum crucible and thermally treated at 1400ºC under an air atmosphere using a heating rate of 1ºC/min with intermediate regrinding to complete the reaction.

2.2 Wet impregnation method

Sm_2GaTaO_7 was impregnated with different content of RuO_2 (0.2, 1.0 and 1.5 weight %) using the stoichiometric amount of ruthenium carbonyl complex, $Ru_3(CO)_{12}$, in tetrahydrofuran. During impregnation, Sm_2GaTaO_7 powders were immersed into solution, the slurry was stirred at 80 ºC until complete evaporation of the solvent. Then, in order to convert the Ru surface species to RuO_2 nanoparticles, each material was thermally treated at 400 ºC by 1 hour under an air atmosphere using a heating rate of 10 °C/min. These materials were labeled as $xRuO_2/Sm_2GaTaO_7$, where "x" denote the weight % impregnated.

2.3 Characterization

Sm_2GaTaO_7 was characterized by X-ray powder diffraction method (XRD) using a Bruker D8 Advance diffractometer and CuKα radiation (λ = 1.5406 Å) as the incident X-ray source. XRD data were collected at room temperature from 10 to 100º with a step interval of 0.01º and a counting time of 1s $step^{-1}$. A detailed analysis of the crystal structure was performed by Rietveld refinement method using TOPAS R3 software [16].

The optical properties were analyzed in the range of 200 – 700 nm at room temperature with a UV–Vis spectrophotometer (Lambda 35 Perkin Elmer Corporation) equipped with an integrating sphere attachment. The energy band gap was determined by Kubelka-Munk function. The morphology and particle size of materials were observed using a JEOL 6490 LV Scanning Electron Microscope (SEM). All samples were stuck to graphite tape and then placed on an aluminum sample holder and located in the SEM chamber. The content of impregnated RuO_2 was determined by energy dispersive X-ray spectroscopy (EDS) analyzing five random zones. The specific surface area (S_{BET}) was determined by physical adsorption of nitrogen at -196 ºC using an analyzer Quantachrome NOVA 2000e. Prior to analysis the samples were degassed at 300 ºC for 1 h.

2.4 Photocatalytic Evaluation

The photocatalytic water splitting reaction was carried out in a reactor with inner quartz cell and a 400 W high pressure mercury lamp as the irradiation source. 0.3 g of photocatalyst was dispersed into 300 mL of pure water under vigorous stirred. Prior to the reaction, argon was bubbled to deaerate the solution. Pressure was set at 100 Torr and temperature was kept at 20 ºC. The amount of hydrogen was analyzed using a chromatograph Varian CP 3380 equipped with a TCD detector and column Hayesep D 100/120 using argon as carrier gas. Reaction evolution was analyzed each 30 minutes during 5 hours.

3. Results and discussion

3.1 Characterization of Sm_2GaTaO_7

According with XRD analysis, Sm_2GaTaO_7 was obtained as a single phase at 1400 ºC and 24 hours. As shown in Figure 1, the diffraction peaks were intensive and narrow, suggesting a good crystallization and large particle size. Sm_2GaTaO_7 was synthesized for the first time, hence there is not standard diffraction pattern for it in the ICDD-PDF (International Centre for Diffraction Data, Powder Diffraction File) database. However, the XRD

pattern obtained for Sm_2GaTaO_7 was quite similar to monoclinic Sm_2FeTaO_7 compound recently reported by our research group [17].

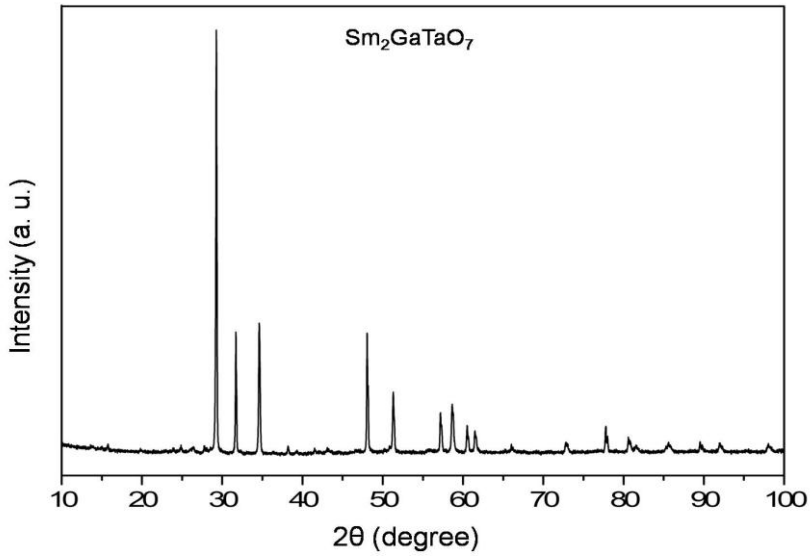

Figure 1. XRD pattern of Sm_2GaTaO_7 synthesized by solid state reaction method at 1400ºC.

To determinate the crystal structure of Sm_2GaTaO_7, a Rietveld refinement was carried out using a theoretical monoclinic unit cell with space group C2/c (No. 15) as a model, recently reported for Sm_2FeTaO_7 [17]. In the model, Ga and Ta ions were assumed to occupy equivalent atomic sites in equal proportion to one another. According to the Rietveld refinement results, experimental and calculated data XRD patterns agreed well with each other, see Figure 2. This means that all X-ray reflections of Sm_2GaTaO_7 can be entirely indexed for a monoclinic crystal structure with the space group C2/c. This results revealed that Sm_2GaTaO_7 and Sm_2FeTaO_7 are isostructural compounds, this is due to their very close ionic radii, Fe^{3+} = 0.64 Å and Ga^{3+} = 0.62 Å [18]. Therefore, Sm_2GaTaO_7 monoclinic structure consists of irregular Ga/Ta octahedra linked at their corners and interconnected into a hexagonal tungsten bronze (HTB)-type network forming 2D HTB blocks, as previously reported for Sm_2FeTaO_7 [17]. The structural arrangement of Sm_2GaTaO_7 differs from $SmTaO_4$ with a fergusonite-type structure that can be regarded as arrays of TaO_4 tetrahedrons that are not linked together [15].

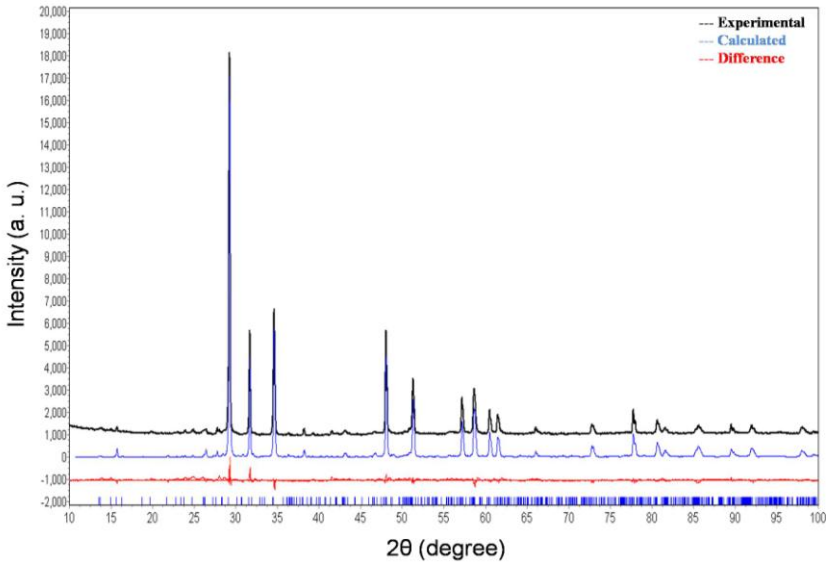

Figure 2. XRD patterns from Rietveld refinement of Sm_2GaTaO_7.

Table 1 shows the crystal data and the reliability factors obtained for Sm_2GaTaO_7, while the refined atomic positions are listed in Table 2. The lattice cell parameters of Sm_2GaTaO_7 are in close agreement to previously reported literature values for similar oxide compounds with monoclinic structure [17,19,20].

Table 1. Crystallographic data obtained from Rietveld refinement results.

Parameter	
a (Å)	13.1386(3)
b (Å)	7.5911(2)
c (Å)	11.5495(3)
β (°)	101.087(2)
Crystal structure	Monoclinic
Space group	C2/c
Z	8
R_{wp}, (%)	6.69
χ^2	1.25

Table 2. Atomic positions of Sm_2GaTaO_7 obtained from Rietveld refinement results.

Atom	Site	Occupancy	x	y	z
Sm1	8(f)	1	0.363(1)	0.129(2)	0.500(1)
Sm2	8(f)	1	0.118(1)	0.135(2)	- 0.009(2)
Ga/Ta1	8(f)	0.5/0.5	0.247(3)	0.111(3)	0.7525(2)
Ga/Ta2	8(f)	0.25/0.25	0.512(4)	0.139(5)	0.292(4)
Ga/Ta3	4(e)	0.5/0.5	0	0.135(3)	0.25
O1	8(f)	1	0.334(3)	0.112(6)	0.306(3)
O2	8(f)	1	0.471(4)	0.128(7)	0.096(3)
O3	8(f)	1	0.218(4)	0.137(6)	0.611(3)
O4	8(f)	1	0.461(3)	0.098(5)	0.726(4)
O5	8(f)	1	0.732(4)	0.142(6)	0.545(3)
O6	8(f)	1	0.031(3)	0.147(6)	0.451(3)
O7	8(f)	1	0.172(2)	0.117(7)	0.762(3)

Figure 3 shows SEM images and EDS spectrum of Sm_2GaTaO_7 and $0.2RuO_2/Sm_2GaTaO_7$ materials. It can be observed that materials exhibit semi-spherical particles with size larger than 1 μm. It could be also observed the presence of particles with neck growths due to sintering process caused by high temperature and long reaction time. The EDS analysis results of RuO_2/Sm_2GaTaO_7 materials revealed that RuO_2 content was 0.2, 0.9 and 1.5 weight percent.

The adsorption analysis results showed that Sm_2GaTaO_7 and RuO_2/Sm_2GaTaO_7 materials had similar specific surface area of around of 0.5 m^2 g^{-1}. This indicates that surface area variation after impregnation was not significant due to the low content of RuO_2 loaded.

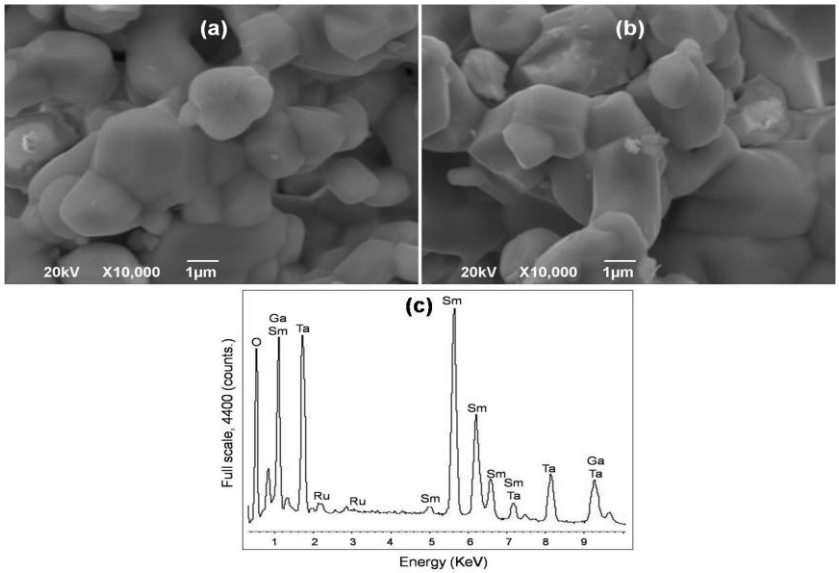

Figure 3. SEM images of Sm_2GaTaO_7 (a), $0.2RuO_2/Sm_2GaTaO_7$ (b) and EDS spectrum of $0.2RuO_2/Sm_2GaTaO_7$.

The UV-Vis diffuse reflectance spectrum of Sm_2GaTaO_7 is showed in Figure 4. The spectrum exhibits the major peak at $\lambda < 320$ nm and also can be noted several peaks at $\lambda > 350$ nm attributed to internal transitions of the partly filled samarium *4f* shell [13,15,21]. According with the Kubelka-Munk analysis results, Sm_2GaTaO_7 possesses an energy band gap (*Eg*) in the order of 4.1 eV. This *Eg* value is comparable to previously reported for similar compounds [15,21].

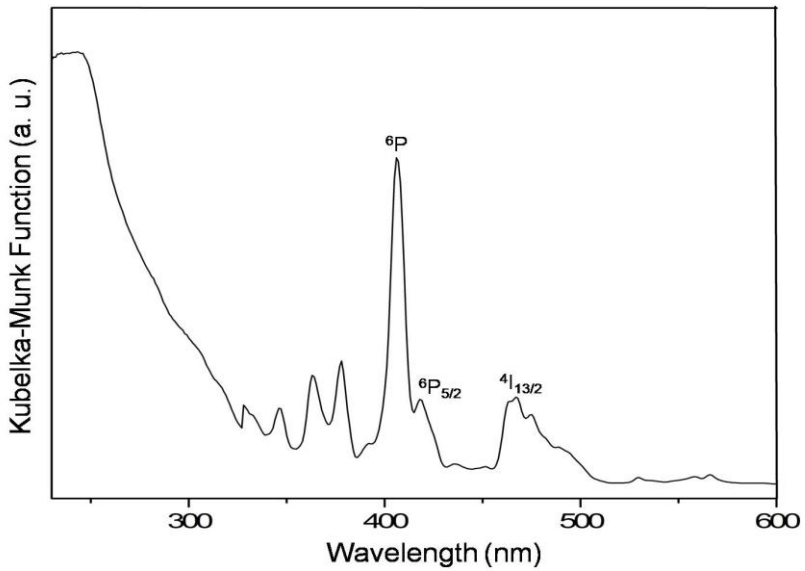

Figure 4. Plot of Kubelka-Munk function of Sm_2GaTaO_7.

Figure 5 shows the UV-Vis diffuse reflectance spectra of Sm_2GaTaO_7 materials. It is evident that the reflectance values gradually decreased (the absorption in opposition increased), as the wt. % RuO_2 amount was increased. After impregnation the samples had a much darker color when RuO_2 content increased, these colored materials necessarily absorbs visible light; which is confirmed by the decreased in reflectance values. These results also confirm the presence of RuO_2 nanoparticles on the Sm_2GaTaO_7 surface.

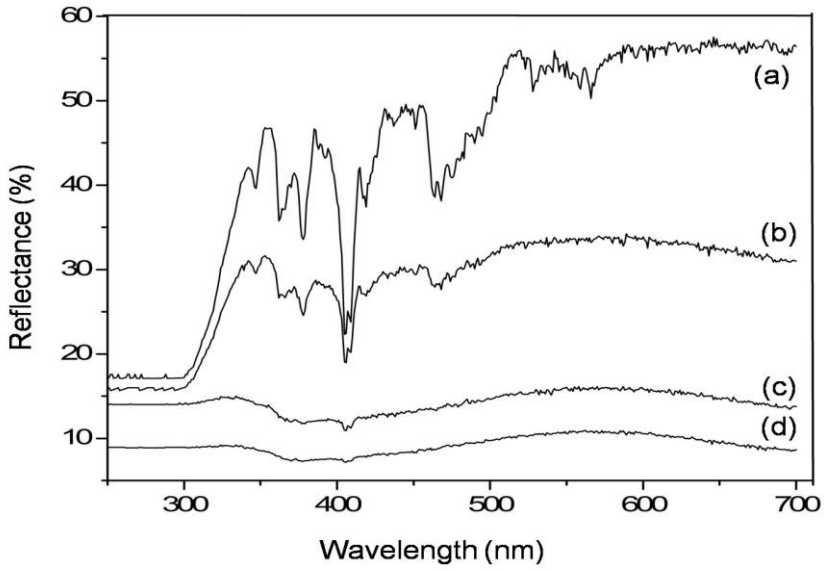

Figure 5. UV-Vis diffuse reflectance spectra of Sm_2GaTaO_7 samples: (a) without RuO_2, (b) 0.2% RuO_2, (c) 0.9% RuO_2 and (d) 1.5% RuO_2.

3.2 Water splitting reaction

Prior the photocatalytic reaction test, blank controls were performed with the same reaction system in dark or in the absence of catalyst. No hydrogen was generated in these conditions. Figure 6 shows the photocatalytic H_2 evolution as a function of irradiation time from pure water. The photocatalytic H_2 evolution are listed in Table 3. Figure 6 shows hydrogen production as function of reaction time. It can be observed that during the first 120 minutes all materials exhibited a similar behavior. After that time, differences can be found in the hydrogen production as function of the RuO_2 wt.% content. The material $0.2RuO_2/Sm_2GaTaO_7$ presents the higher hydrogen production but when the RuO_2 amount increase to 0.9 and 1.5 wt.%, hydrogen production decreases considerably and it is even less than Sm_2GaTaO_7. These results revealed that RuO_2 as cocatalyst provide efficient active sites for H_2 evolution, however an excess in the RuO_2 wt. % amount may cause agglomeration of the RuO_2 nanoparticles reducing the number of active sites for H_2 evolution. Moreover, excessively loaded of RuO_2 hinder light absorption by the base photocatalysts reducing the generation of the electron-hole pair and in some cases could act as recombination centers [1].

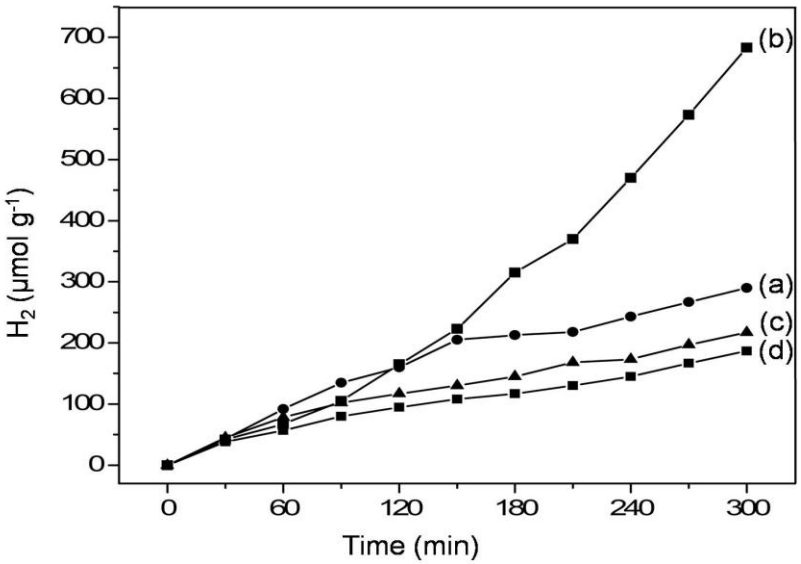

Figure 6. Photocatalytic hydrogen production of Sm_2GaTaO_7 materials: (a) without RuO_2, (b) 0.2% RuO_2, (c) 0.9% RuO_2 and (d) 1.5% RuO_2.

Table 3. Photocatalytic activity of Sm_2GaTaO_7 for hydrogen production

Photocatalyst	**H_2 evolution (μmol h^{-1} g^{-1})**
Sm_2GaTaO_7	58
$0.2RuO_2/Sm_2GaTaO_7$	137
$0.9RuO_2/Sm_2GaTaO_7$	43
$1.5RuO_2/Sm_2GaTaO_7$	37

Although it has been reported that RuO_2 cocatalyst can act as both reduction and oxidation site during water splitting reaction [5]. However, in the present work, it was observed that RuO_2 only acts as reduction site for H_2 evolution because O_2 evolution was not presented. It could be associated with the possible adsorption of O_2 molecules onto the Sm_2GaTaO_7 surface. These was previously reported by some authors [13,22].

Table 4 resumes some H_2 production reported results. In most of the cases, the H_2 production obtained in this work is superior than many of these studies under similar reaction conditions even some of the reported works used sacrificial agents such as methanol and ethanol that under certain condition, they can also undergo photocatalytic reforming to produce hydrogen. This implies that, using an alcohol solution, the origin of the produced H_2 is uncertain and may not be issued exclusively from photocatalytic water splitting [23-25]. The H_2 production rate of Sm_2GaTaO_7 was 39 times higher than $SmTaO_4$ under similar reaction conditions. This higher hydrogen production can be understood from the following aspects. Firstly, the presence of Ga^{3+} makes possible the formation of a 4f-d^{10}-d^0 electronic configuration compound which favors the mobility of the electron-hole pairs [13]. The second one is related with the crystal structure arrangement of Ga/Ta octahedral. The presence of two metals ions with different electronic configuration at the same crystalline site of the Sm_2GaTaO_7 structure

arrangement generate the formation of highly distorted octahedral units facilitating the generation and mobility to the surface of the photogenerated electron-hole pairs. And finally, the use of RuO_2 as cocatalyst decreases considerably the recombination of the electron-hole pairs and provides extra reaction sites for the H_2 evolution. Therefore, Sm_2GaTaO_7 in combination with an optimal amount of RuO_2 as cocatalyst can be considered an attractive material for pure water splitting. This information might be useful for designing new photocatalyst materials for water splitting.

Table 4. Comparative results of specific H_2 evolution from photocatalytic water splitting using different complex oxides

Photocatalyst	Sacrificial agent	Reaction conditions	Light source	Specific H_2 evolution ($\mu mol\ h^{-1}\ g^{-1}$)	Ref.
Sm_2GaTaO_7 0.2 RuO_2/Sm_2GaTaO_7	none	0.3 g of catalyst and 300 mL of pure water	400 W High Pressure Hg lamp	58 137	This work
$SmTaO_4$ 0.7 $Ni/SmTaO_4$	none	0.2 g of catalyst and 200 mL of pure water	400 W High Pressure Hg lamp	1.5 46	15
$RbSmTa_2O_7$	none	0.2 g of catalyst and 200 of mL pure water	400 W High Pressure Hg lamp	53	21
0.2 Pt/Bi_2GaTaO_7 0.2 Pt/Bi_2InTaO_7 0.2 Pt/Bi_2FeTaO_7	methanol	2 g of catalyst, 50 mL of methanol and 320 mL of water	400 W High Pressure Hg lamp	31 497 56	26
Bi_2LaTaO_7 Bi_2YTaO_7	none	1 g of catalyst and 300 mL of pure water	400 W High Pressure Hg lamp	42 34	27
Bi_2AlNbO_7 NiO_x/Bi_2AlNbO_7 $Bi_{1.8}La_{0.2}AlNbO_7$ $NiO_x/Bi_{1.8}La_{0.2}AlNbO_7$	methanol	0.1 g of catalyst, 20 mL of methanol and 400 mL of water	350 W High Pressure Hg lamp	45 74 105 141	28
$La:Cd_2TaGaO_6$ $0.5Pt/La:Cd_2TaGaO_6$ $0.5NiO/La:Cd_2TaGaO_6$	ethanol	0.3 g of catalyst, 45 mL of ethanol and 405 mL of water	300 W High Pressure Hg lamp	300 5700 2833	7

4. Conclusions

The Sm_2GaTaO_7 was synthesized for the first time through solid state reaction. The XRD results indicate that the compound crystallized in the monoclinic system with a space group C2/c. The Sm_2GaTaO_7 was able to produce H_2 from pure water, this result reveals that crystal structure and the constitute elements play an important role in the photocatalytic activity. The RuO_2 acts as an effective cocatalyst to enhance photocatalytic H_2 production activity of Sm_2GaTaO_7. The optimal RuO_2 loading amount was found to be 0.2 wt.%. At this content, H_2 production was 137 $\mu mol\ h^{-1}\ g^{-1}$, which exceeded 2.4 times the production of pure Sm_2GaTaO_7.

5. Acknowledgements

Authors want to thank for the financial support of this research to CONACYT through project CB 98740-2008 as well as PAICYT-UANL-2010 projects and PIFI-2011. Miguel A. Ruiz-Gómez would like to thank CONACYT for his scholarship no. 239336.

6. References

[1] K. Maeda, J. Photochem. Photobiol., C, 12, 237 (2011).

[2] D. Jing, L. Guo, L. Zhao, X. Zhang, H. Liu, et al., Int. J. Hydrogen Energy, 35, 7087 (2010).

[3] J. Zhu and M. Zach, Curr. Opin. Colloid Interface Sci., 14, 260 (2009).

[4] A. Kudo and Y. Miseki, Chem. Soc. Rev., 38, 253 (2009).

[5] K. Maeda, R. Abe and K. Domen, J. Phys. Chem. C, 115, 3057 (2011).

[6] L.M. Torres-Martínez, R. Gómez, O. Vázquez-Cuchillo, I. Juárez-Ramírez, A. Cruz-López and F.J. Alejandre-Sandoval, Catal. Commun., 12, 268 (2010).

[7] Y. Chen, H. Yang, X. Liu and L. Guo, Int. J. Hydrogen Energy, 35, 7029 (2010).

[8] I.S. Cho, S.T. Bae, D.H. Kim and K.S. Hong, Int. J. Hydrogen Energy, 35, 12954 (2010).

[9] J. Sato, N. Saito, H. Nishiyama and Y. Inoue, J. Phys. Chem. B, 105, 6061 (2001).

[10] J. Sato, H. Kobayashi, K. Ikarashi, N. Saito, H. Nishiyama and Y. Inoue, J. Phys. Chem. B, 108, 4369 (2004).

[11] N. Arai, N. Saito, H. Nishiyama, Y. Shimodaira, H. Kobayashi, Y. Inoue and K. Sato, J. Phys. Chem. C, 112, 5000 (2008).

[12] X.D. Tang, H.Q. Ye, H. Liu, C.X. Ma and Z. Zhao, Chem. Phys. Lett., 484, 48 (2009).

[13] X. Tang, H. Ye, H. Liu, C.X. Ma and Z. Zhao, J. Solid State Chem., 183, 192 (2010).

[14] R. Abe, M. Higashi, Z. Zou, K. Sayama, Y. Abe and H. Arakawa, J. Phys. Chem. B, 108, 811 (2004).

[15] M. Machida, S. Murakami, T. Kijima, S. Matsushima and M. Arai, J. Phys. Chem. B, 105, 3289 (2001).

[16] Software Topas R, version 3, Bruker AXS, West Germany, (2005).

[17] L.M. Torres-Martínez, M.A. Ruiz-Gómez, M.Z. Figueroa-Torres, I. Juárez-Ramírez, E. Moctezuma and E. López-Cuellar, Mater. Chem. Phys., 133, 839 (2012).

[18] R.D. Shannon, Acta Cryst., 32, 751 (1976).

[19] G.M. Veith, M.V. Lobanov, T.J. Emge, M. Greenblatt, F. Stowasser, et al., J. Mater. Chem., 14, 1623 (2004).

[20] I. Levin, T.G. Amos, J.C. Nino, T.A. Vanderah, I.M. Reaney, C.A. Randall and M.T. Lanagan, J. Mater. Res., 17, 1406 (2002).

[21] M. Machida, J. Yabunaka and T. Kijima, Chem. Mater., 12, 812 (2000).

[22] J. Yin, Z. Zou and J. Ye, J. Phys. Chem. B, 107, 4936 (2003).

[23] O. Rosseler, M.V. Shanker, M. K. Du, L. Schmidlin, N. Keller and V. Keller, J. Catal., 269, 179 (2010).

[24] T. Puangpetch, T. Sreethawong, S. Yoshikawa and S. Chavadej, J. Mol. Catal. A: Chem., 312, 97 (2009).

[25] J. Wang, C.S. Lee and M.C. Lin, J. Phys. Chem. C, 113, 6681 (2009).

[26] J. Wang, Z. Zou and J. Ye, J. Phys. Chem. Solids, 66, 349 (2005).

[27] J. Luan, X. Hao, S. Zheng, G. Luan and X. Wu, J. Mater. Sci., 41, 8001 (2006).

[28] Y. Li, G. Chen, H. Zhang and Z. Li, Mater. Res. Bull., 44, 741 (2009).